

Unification of quantum Zeno-anti Zeno effects and parity-time symmetry breaking transitions

Jiaming Li,* Tishuo Wang, and Le Luo†

School of Physics and Astronomy, Sun Yat-Sen University, Zhuhai, Guangdong, China 519082

Sreya Vemuri and Yogesh N Joglekar

Department of Physics, Indiana University Purdue University Indianapolis (IUPUI), Indianapolis, Indiana 46202, USA

(Dated: April 6, 2020)

The decay of any unstable quantum state can be inhibited or enhanced by carefully tailored measurements, known as the quantum Zeno effect (QZE) or anti-Zeno effect (QAZE). To date, studies of QZE (QAZE) transitions have since expanded to various system-environment coupling, in which the time evolution can be suppressed (enhanced) not only by projective measurement but also through dissipation processes. However, a general criterion, which could extend to arbitrary dissipation strength and periodicity, is still lacking. In this letter, we show a general framework to unify QZE-QAZE effects and parity-time (\mathcal{PT}) symmetry breaking transitions, in which the dissipative Hamiltonian associated to the measurement effect is mapped onto a \mathcal{PT} -symmetric non-Hermitian Hamiltonian, thus applying the \mathcal{PT} symmetry transitions to distinguish QZE (QAZE) and their crossover behavior. As a concrete example, we show that, in a two-level system periodically coupled to a dissipative environment, QZE starts at an exceptional point (EP), which separates the \mathcal{PT} -symmetric (PTS) phase and \mathcal{PT} -symmetry broken (PTB) phase, and ends at the resonance point (RP) of the maximum \mathcal{PT} -symmetry breaking; while QAZE extends the rest of PTB phase and remains the whole PTS phase. Such findings reveal a hidden relation between QZE-QAZE and PTS-PTB phases in non-Hermitian quantum dynamics.

Quantum Zeno (anti-Zeno) effect is an important feature of a quantum system, initially interpreted as that the evolution of the system can be suppressed (enhanced) by measuring it frequently enough in its known initial state [1–10]. As an outgrowth of study of the QZE (QAZE), they have been extensively used to control and manipulate quantum systems, including changing the decay rate of an unstable state [3, 11–13], protecting quantum information [14], suppressing decoherence [8, 15], extending the lifetime of ultracold molecular [16], and suppressing the tunneling in an optical lattice [11, 17, 18].

The meaning of QZE (QAZE) terms have since expanded, in which the time evolution can be suppressed (enhanced) not only by projective measurement but also by a variety of dissipation processes. Along this line, a non-Hermitian term of dissipation $-i\gamma$ is inserted into the Hermitian dynamics of the unstable system for pulling away the curtain that hides the measurement process [19, 20]. Such non-Hermitian Hamiltonians are equivalent to the multi-mode Jaynes-Cummings model that includes the coupling between the system and the measurement “apparatus”, enabling a unified theory to describe QZE (QAZE) through both repetitive and continuous observations.

It is still an open question how to describe both measurement effect and dissipation process so that deceleration (QZE) and acceleration (QAZE) of the evolution of a quantum system can be justified by a simple criterion. In Ref. [21], such criterion had been established for the case of frequent projective measurement, in which the modified decay rate is simply determined by the overlap of the reservoir coupling spectrum and the broadening spec-

trum of the level that is frequently measured. However, a general criterion, which could extend to dissipation with arbitrary small strength, is still lacking. Such extension is not trivial, as explained in Ref. [21], the effect of projective measurement is treated as phase randomization and induce level broadening consequently. For small dissipation, we then need to deal with partial decoherence which could induce the nontrivial broadening of the quantum level described by a stochastic, non-linear Liouville equation [22]. Moreover, it is quite interesting to find out the dependence of the strength of QZE (QAZE) on the realistic parameters, especially at the limit of small dissipation strength and arbitrary sequences, where the modified time evolution usually do not behave as expected for idealized projective measurements.

Recently, emerging studies in passive \mathcal{PT} -symmetric quantum systems indicate the appearance of a slow decay mode associated with the PTB phase [23–26]. Based on these discoveries, in this letter, we unify QZE (QAZE) and \mathcal{PT} symmetry breaking transitions in non-Hermitian quantum mechanics, and find \mathcal{PT} symmetry breaking transitions play a general role in determining QZE (QAZE) in open quantum systems. This treatment enables us to search for QZE (QAZE) behaviors by analyzing the phase diagram of a \mathcal{PT} symmetric non-Hermitian Hamiltonian. We explicitly show that \mathcal{PT} symmetry transitions hidden in a pure lossy two-level system could be used for characterizing QZE (QAZE) precisely with arbitrary dissipation strength and period.

The relation between QZE (QAZE) and \mathcal{PT} -symmetry transition is built as follows: First, the projective measurement related to QZE (QAZE) is considered as a pure

loss term that couples the system to the environment at the strong limit of dissipation strength. Then, by decreasing the dissipation strength, QZE (QAZE) is studied in the weak dissipation regime. This non-Hermitian Hamiltonian is given by

$$H = \omega_0|1\rangle\langle 1| + (\omega - 2i\gamma)a^\dagger a + a^\dagger \Phi|0\rangle\langle 1| + a\Phi^*|1\rangle\langle 0|, \quad (1)$$

which describe a system that an atom in the excited state $|1\rangle$ of energy ω_0 decays to the ground state of zero energy by emitting photons, falling in a single photon mode with frequency ω . We model the action of the measurement by considering that the state to which $|1\rangle$ decays is itself unstable with a decay rate γ [19]. Second, the pure dissipative Hamiltonian associated to QZE (QAZE) can be mapped into a balanced gain-loss Hamiltonian with \mathcal{PT} symmetry. Defining $\omega_a = (\omega_0 + \omega)/2$ and $\Delta = (\omega_0 - \omega)/2$, we have $H = H_0 + H_{int}$, where $H_0 = (-i\gamma + \omega_a)\mathbb{1} + \Delta\sigma_z$ with $\mathbb{1}$ is the unit matrix and σ_z the Pauli matrix, and we have

$$H_{int} = \begin{pmatrix} +i\gamma & \Phi^* \\ \Phi & -i\gamma \end{pmatrix} \quad (2)$$

$H_{int} = \mathcal{PT}H_{int}\mathcal{PT}$ is a balanced gain-loss Hamiltonian H_{PT} remaining invariant under \mathcal{PT} operation with the parity operator given by $\mathcal{P} = \sigma_x$ and the antilinear time-reversal operator given by $\mathcal{T}i\mathcal{T} = -i$. This \mathcal{PT} -symmetric Hamiltonian allows phase transitions in its eigenvalue spectrum, where the eigenvalue changes from purely real to complex-conjugate pairs. Known as passive \mathcal{PT} -symmetry transitions, the transitions of a no-gain system with mode-selective losses has been successfully observed in various systems [23, 25–39]. Third, we adopt the frequency-dependent method to signal the QZE (QAZE) [40–43]. In the frequency-dependent picture, QZE(QAZE) is defined in such a way that the effective decay rate $\Gamma(\omega)$ decreases (increases) as the measurement (dissipation) frequency ω increases. This definition provides a clear physical picture: the rapidly repeated measurements suppressed (enhanced) the relaxation process of the unstable state, thus leading to the QZE (QAZE).

Based on these ideas, we put our focus on analyzing how the strength and periodicity of the dissipation term γ play a role in the decay rate Γ of an unstable system, especially on the slow decay mode that could induce QZE (QAZE) when tuning the strength or frequency of the dissipation. For a static dissipation, at small dissipation strength, the decay rate of the system $\Gamma(\gamma_0)$ increases as γ_0 , whereas the decay rate could be slowed down by increasing γ_0 at larger strength. For a time-periodically modulated dissipation $\Gamma(\omega)$, the decay rate depends on both the magnitude of the dissipation and its modulation frequency, leading to a rich phase diagram separated by multiple PTS and PTB phases [23, 44]. In the PTS phase, the decay rate always increases as the

increase of the dissipation frequency. In contrast, the eigenvalues have two branches in the PTB phase, one is the “slow mode” with less imaginary(loss) components than the other “fast mode”. While the fast mode decays quickly, the slow mode survives in the longer time and dominate the time evolution so that the effective decay rate is slowed down.

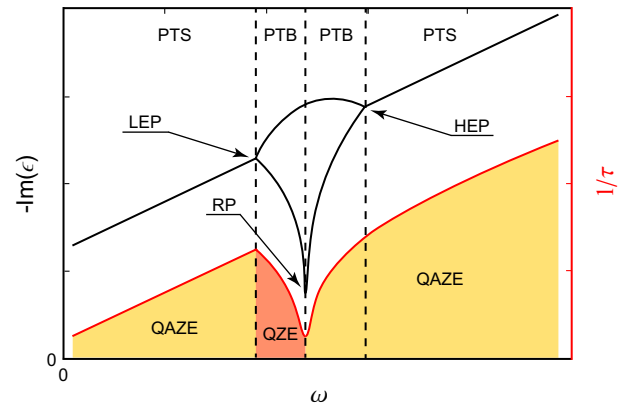


FIG. 1. The concept picture indicating the relation between QZE (QAZE) and \mathcal{PT} -symmetry breaking transitions. Black solid line: the dependence of the imaginary part of the quasienergy $-\text{Im}(\epsilon)$ of a passive \mathcal{PT} -symmetry Hamiltonian on the frequency of the dissipation ω . Red solid line: The effective decay rate of an unstable system with the characteristic life time τ . QZE (QAZE) represents for quantum zero (anti-zero) effect. PTS (PTB) represents for \mathcal{PT} -symmetric (\mathcal{PT} -symmetry broken) phase. LEP(HEP) is the exceptional point of \mathcal{PT} -symmetry breaking transitions with PTS at low (high) frequency side. RP is the resonant point of the PTB phase.

It is naturally to ask if a PTB phase corresponds to QZE while a PTS phase to QAZE. The answer is that the direct correspondence is not valid. Instead, we present a general relation shown in Fig. 1 by analyzing the dependence of the imaginary part of the eigenvalues on the frequency of the dissipation. In the PTS phase, the imaginary part of the eigenvalue increases as the dissipation frequency ω becomes larger, so that QAZE will be observed. When the dissipation frequency is larger than the LEP, the “slow mode” of the eigenvalue appears and the imaginary part of “slow mode” decreases as ω increases. In the PTB regime, the decay rate of the system is dominated by the “slow mode” which inhibits the decay, indicating QZE until ω increases to the RP. Above that, the imaginary part of “slow mode” increases as ω increases, showing QAZE. The QAZE exists in the PTB phase that is above the resonant point, and remains in the PTS phase while ω increases and passed the HEP. This analysis uses the frequency response of a decay system to define QZE (QAZE) and depends on the eigengmode behavior of a passive \mathcal{PT} -symmetric system. These ar-

guments are rather general not depending on the details of Hamiltonian, so we think this is a universal relation to unify parity-time symmetry breaking transitions of a non-Hermitian Hamiltonian and QZE (QAZE) in open quantum systems.

To make physics clear in a simple context, we illustrate the above relation using a two-level dissipative Rabi system driven by the resonant photon mode $H_L = -J(t)(|\uparrow\rangle\langle\downarrow| + |\downarrow\rangle\langle\uparrow|) - 2i\gamma(t)|\downarrow\rangle\langle\downarrow|$, in which the coupling rate $J(t)$ and the dissipation rate $\gamma(t)$ of the $|\downarrow\rangle$ -level are both time dependent. As shown in Eq. 2, this Hamiltonian can be written as $H_L = -i\gamma\mathbb{1} + H_{PT}$.

To reveal QZE (QAZE), J_0 is constant, and a square-wave modulation of the dissipation $\gamma(t)$ with pulse width τ_1 and period T is applied

$$\gamma(t) = \begin{cases} \gamma_0 & 0 \leq t < \tau_1, \\ 0 & \tau_1 \leq t < T, \end{cases} \quad (3)$$

where $T = 2\pi/\omega$ is the period of the Hamiltonian i.e. $H_L(t + T) = H_L(t)$. The PTS (PTB) phases are defined via quasienergies ϵ_F^\pm of the effective Floquet Hamiltonian H_L , which are obtained from the eigenvalues of the non-unitary time evolution operator for one period $G'(T)$ (see Supplementary Materials A). Here $G'(T) = e^{-iH_L(T-\tau_1)}e^{-iH_L\tau_1} = e^{-\gamma_0\tau_1}G(T)$ with $G(T) = e^{-iH_{PT}(T-\tau_1)}e^{-iH_{PT}\tau_1}$ as the time evolution operator of balanced gain and loss. ϵ_F^\pm is then given by

$$\epsilon_F^\pm = -i\gamma_0\tau_1/T + i\ln(\Lambda_F^\pm)/T \quad (4)$$

with Λ_F^\pm of the eigenvalue of $G(T)$,

$$\Lambda_F^\pm = c_1c_2 - \frac{J_0}{\epsilon_0}s_1s_2 \pm \sqrt{\left(\frac{\gamma_0}{\epsilon_0}s_1\right)^2 - \left(c_1s_2 + \frac{J_0}{\epsilon_0}s_1s_2\right)^2}. \quad (5)$$

The parameters are defined as $c_1 \equiv \cosh(\epsilon_0\tau_1)$, $c_2 \equiv \cos[J_0(T-\tau_1)]$, $s_1 \equiv \sinh(\epsilon_0\tau_1)$, $s_2 \equiv \sin[J_0(T-\tau_1)]$ and $\epsilon_0 \equiv \sqrt{\gamma_0^2 - J_0^2}$.

The imaginary parts of the quasi-energies $\epsilon_F^\pm(\gamma_0, \omega, \tau_1)$ determine the decay rates $\Gamma_F^\pm = -2\text{Im}\epsilon_F^\pm$. In the PTS phase, Λ_F^\pm are complex conjugates of each other and have the same magnitude. Therefore, the real part of $\ln \Lambda_F^\pm$ are the same, so does the imaginary part of ϵ_F^\pm . Thus the decay rates Γ_F^\pm are equal and increase when γ_0 increases. In the PTB phase, both Λ_F^\pm become purely real, leading to the imaginary parts of ϵ_F^\pm different and the emergence of two different decay rates, named as ‘‘slow mode’’ and ‘‘fast mode’’. Two modes arises at the exceptional point of the \mathcal{PT} symmetry breaking transition. The degree of symmetry breaking is described by a dimensionless parameter $\mu(\gamma_0, \omega) = ||e^{-i\epsilon_F^+T}| - |e^{-i\epsilon_F^-T}||$. As an example, Figure 2(a) shows $\mu(\gamma_0, \omega)$ for dissipation with the pulse parameter of $J_0\tau_1 = 0.01$, and Figure 2(b) shows the decay rates Γ_F obtained along the red-dash line in

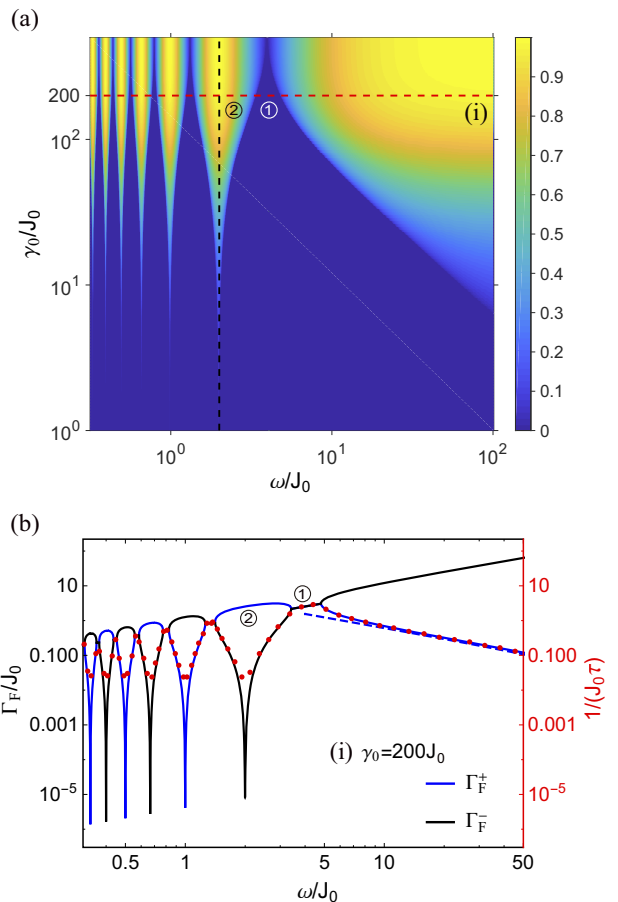


FIG. 2. The decay rates of a two-level system with a time-dependent dissipation modeled by \mathcal{PT} -symmetric Hamiltonian. (a) The phase diagram of \mathcal{PT} symmetry breaking, in which the color presents $\mu(\gamma_0, \omega)$. The vertical axis is the normalized dissipation amplitude γ_0/J_0 , and the horizontal axis is normalized modulation frequency ω/J_0 . Note that the phase diagram is obtained by fixing τ_1 and varying T . Although the widths of the PTS phases (deep blue color) and PTB phases (all other colors) depend on τ_1 , the structure of the phase diagram as well as the location of the resonance peaks (one of them represented by the black-dash line) does not depend on τ_1 . (b) The comparison of the decay rates Γ_F and the lifetime τ along the red-dash line in Fig 2(a) with $\gamma_0 = 200J_0$. The red dot is the numerical simulation of the lifetime of the unstable state. ① (②) presents one of the PTS (PTB) regime.

Fig 2(a). The coincidence between the lifetime of the unstable state and the decay rates of the eigenmodes have been confirmed from large to small dissipation strength (Supplementary Materials C).

We could extend this result to the whole \mathcal{PT} phase diagram as shown in Fig. 2. There are multiple PTS and PTB blocks with the resonant frequencies of PTB as $\omega_n/J_0 = 2/n$, where $n = 1, 2, 3, \dots$ (see Supplementary Materials B). In one of the PTS blocks (marked as ①)

shown in Fig. 2, Γ_F^\pm decreases with the decreases of the modulation frequency, indicates QAZE. As the modulation frequency decreases, the system experiences a phase transitions from the PTS to PTB. After crossing the exceptional point, in one of the PTB blocks (marked as ②), the decay rate of the slow mode is not monotonous. Below the PTB resonance, the Γ_F^- decreases with the increase of ω and reverses trend above the resonance, so both the QZE and QAZE appear in the PTB phase, and the transition from the QAZE to the QZE is determined by ω_n .

This framework leads to the unification of the \mathcal{PT} symmetry braking transition and QAZ(QAZE). But does this unification also support the results of the projective measurements and continuous observation (static dissipation)? The answer is yes, and we confirm that the universality of this unification is applied for both cases.

First, projective measurements. For comparing with QZE(QAZE) induced by projective measurements, we need to consider the limit of the large and frequent dissipation with $\gamma_0/J_0 \gg 1$ and $\omega/J_0 \gg 1$, the decay rate of the states Γ_F^\pm is simplified as $\Gamma_F^\pm = (J_0^2/\gamma_0)(\tau_1/T) + 2 \ln((c_2 \pm \sqrt{1-s_2^2})/2)/T$. With $\omega/J_0 \gg 1$, $\cos(J_0\tau_2) \rightarrow e^{-(J_0\tau_2)^2/2}$, we got

$$\Gamma_F^\pm = \frac{J_0^2}{\gamma_0} \frac{\tau_1}{T} + J_0^2 \frac{\tau_2^2}{T} \quad (6)$$

On the other hand, a two-level system in which the projective measurements applied to the final state allows QZE [8], in which the two-level system is driven at Rabi frequency ω_R with the initial population of the atoms in the $|\uparrow\rangle$, while the final dissipative state $|\downarrow\rangle$ has a decay rate γ_c coupled to the third state. When N rapid projective measurements with time intervals of $\delta t = t/N$ are applied the final state, the survival probability of the initial state after N times measurements is $p^N(t) = p(\delta t)^N \simeq [1 - (\omega_R \delta t/2)^2]^N$. When $\delta t \ll \pi/\omega_R$, the decay rate of $p^N(t)$ is $1/\tau_{QZE} = \omega_R^2 \delta t/4$, showing that the projective measurements slow down the decay of the state. In the real experiments, the measurement time is finite, both the measurement pulse duration t_p and the time interval between the two consecutive pulses δt are needed to be considered, giving the decay rate

$$\frac{1}{\tau} = \frac{\omega_R^2}{\gamma_c} \frac{t_p}{t_p + \delta t} + \frac{\omega_R^2}{4} \frac{\delta t^2}{t_p + \delta t} \quad (7)$$

It is obvious that Eq. 6 and Eq. 7 are equivalent, which indicates that QZE(QAZE) can be well understood in terms of the picture of \mathcal{PT} symmetry breaking transition. The blue-dash line in Fig. 2 (b) is plot as Eq. 7, showing that the two decay rates are in agreement with each other very well.

Second, continuous observation (static dissipation). In the static case, the eigenvalues are given by $\lambda_\pm = -i\gamma_0 \pm \sqrt{J_0^2 - \gamma_0^2}$ where J_0, γ_0 are the static parameters.

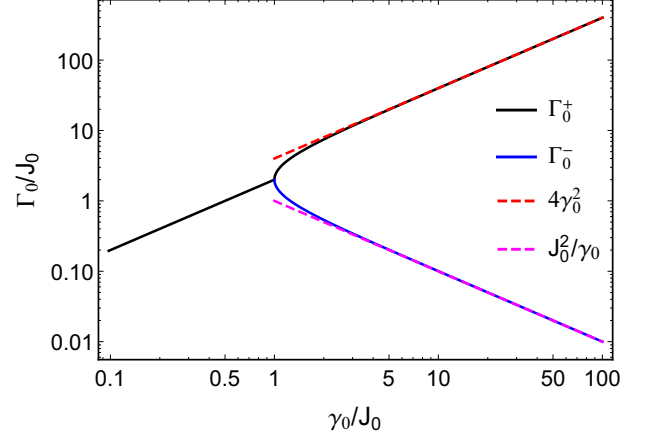


FIG. 3. The decay rates of continuous observation as a function of the static dissipation. The black (blue) lines present the two eigenmode Γ_0^+ (Γ_0^-) in the PTB phase respectively (the two eigenmodes overlap in the PTS phase). The dashed lines present the decay rates at the limit of $\gamma_0 \gg J_0$.

The decay rates Γ_0^\pm as a function of γ_0/J_0 is shown in Fig. 3. When $\gamma_0 \leq J_0$ with the J_0 as the LEP, the system is in the PTS phase and the decay rates of the two eigenmodes are equal, $\Gamma_0^\pm = 2\gamma_0$. In this phase, the decay rate increases as γ_0 increases. When $\gamma_0 > J_0$, the system is in the PTB phase, leading to the emergence of two modes given by

$$\begin{aligned} \Gamma_0^- &= 2(\gamma_0 - \sqrt{\gamma_0^2 - J_0^2}) \xrightarrow{\gamma_0 \gg J_0} \frac{J_0^2}{\gamma_0}, \\ \Gamma_0^+ &= 2(\gamma_0 + \sqrt{\gamma_0^2 - J_0^2}) \xrightarrow{\gamma_0 \gg J_0} 4\gamma_0. \end{aligned} \quad (8)$$

In the limit $\gamma_0 \gg J_0$, the decay rate for the “fast mode” doubles, $\Gamma_0^+ \rightarrow 4\gamma_0$, whereas that for the “slow mode” vanishes, $\Gamma_0^- \rightarrow J_0^2/\gamma_0$. These values coincide the continuous QZE case with theory in Ref. [19] and experiment in Ref. [8]. The populations of up and down levels decays are given by $1/\tau_{|\uparrow\rangle} = \omega_R^2/\gamma_c$ and $1/\tau_{|\downarrow\rangle} = \gamma_c$ from the picture of quantum measurement. It is clear that the two approaches are equivalent provided $\omega_R = 2J_0$ and $\gamma_c = 4\gamma_0$. In the strong-dissipation limit $\gamma_0 \gg J_0$, the slowly-decaying eigenmode has a near-unity overlap with the $|\uparrow\rangle$, while the rapidly-decaying eigenmode is mostly aligned with $|\downarrow\rangle$. Thus, the PTB phase provides a suitable generalization of the continuous QZE when the dissipation strength is moderate, $\gamma_0 \gtrsim J_0$. On the other hand, when $\gamma_0 \leq J_0$, the two decay rates $\Gamma_0^\pm = 2\gamma_0$ increase with increasing dissipation, which is consistent with the QAZE.

We formulate a general picture of QZE(QAZE) in the two-level dissipative Rabi system based on the phase diagram of \mathcal{PT} symmetry. QZE is always observed, above certain modulation frequency ω , in the strong dissipative

regime $\gamma_0/J_0 \gg 1$. But, even deep in the strong dissipation regime, QAZE could also be observed around specific modulation frequencies near the EP points. On the other hand, at small dissipation strengths, QAZE can be observed at most modulation frequencies. Conversely, the QZE regime survives down to vanishingly small dissipation strengths, i.e. $\gamma_0/J_0 \ll 1$, only with the modulation frequencies in the range between the LEP and the RP of the PTB phase.

In conclusion, we unify the symmetry transitions associated to \mathcal{PT} -symmetric non-Hermitian Hamiltonians with quantum measurement effect of QZE (QAZE). Using a dissipation term, instead of projective measurement, the interaction between the unstable system and the environment can be either strong or weak, enabling a systematic study of weak dissipation, in which QZE(QAZE) will not be as manifest as in the projective measurement case. We find that \mathcal{PT} phase transitions exit in all types of QZE(QAZE) effects whether the dissipation is strong or weak, periodically or static. Such findings helps to explore QZE(QAZE) physics in more complex setups, such as beyond Markovian approximation [45, 46] and with many-body interactions [47, 48], with a simple, quantitative criterion, leading further studies of the deep relations between quantum measurement effects and the dynamics of non-Hermitian open systems.

JLi received supports from National Natural Science Foundation of China (NSFC) under Grant No.11804406, Fundamental Research Funds for Sun Yat-sen University, Science and Technology Program of Guangzhou 2019-030105-3001-0035. YNJ was supported by NSF grant DMR-1054020. LL received supports from NSFC under Grant No.11774436, Guangdong Province Youth Talent Program under Grant No.2017GC010656, Sun Yat-sen University Core Technology Development Fund, and the Key-Area Research and Development Program of Guangdong Province under Grant No.2019B030330001.

* lijiam29@mail.sysu.edu.cn

† luole5@mail.sysu.edu.cn

- [1] B. Misra and E. G. Sudarshan, *J. Math. Phys.* **18**, 756 (1977).
- [2] W. Schieve, L. Horwitz, and J. Levitan, *Phys. Lett. A* **136**, 264 (1989).
- [3] W. M. Itano, D. J. Heinzen, J. J. Bollinger, and D. J. Wineland, *Phys. Rev. A* **41**, 2295 (1990).
- [4] D. Home and M. Whitaker, *Ann. Phys.* **258**, 237 (1997).
- [5] B. Kaulakys and V. Gontis, *Phys. Rev. A* **56**, 1131 (1997).
- [6] P. Facchi, V. Gorini, G. Marmo, S. Pascazio, and E. Sudarshan, *Phys. Lett. A* **275**, 12 (2000).
- [7] M. Lewenstein and K. Rzażewski, *Phys. Rev. A* **61**, 022105 (2000).
- [8] E. W. Streed, J. Mun, M. Boyd, G. K. Campbell, P. Medley, W. Ketterle, and D. E. Pritchard, *Phys. Rev. Lett.* **97**, 260402 (2006).
- [9] P. Facchi, H. Nakazato, and S. Pascazio, *Phys. Rev. Lett.* **86**, 2699 (2001).
- [10] P. Facchi and M. Ligab, *J. Math. Phys.* **51**, 022103 (2010).
- [11] M. C. Fischer, B. Gutiérrez-Medina, and M. G. Raizen, *Phys. Rev. Lett.* **87**, 040402 (2001).
- [12] B. Yan, S. A. Moses, B. Gadway, J. P. Covey, K. R. Hazzard, A. M. Rey, D. S. Jin, and J. Ye, *Nature* **501**, 521 (2013).
- [13] M.-C. Zhang, W. Wu, L.-Z. He, Y. Xie, C.-W. Wu, Q. Li, and P.-X. Chen, *Chin. Phys. B* **27**, 090305 (2018).
- [14] S. Hacoheh-Gourgy, L. P. Garcia-Pintos, L. S. Martin, J. Dressel, and I. Siddiqi, *Phys. Rev. Lett.* **120**, 020505 (2018).
- [15] J. M. Raimond, P. Facchi, B. Peaudecerf, S. Pascazio, C. Sayrin, I. Dotsenko, S. Gleyzes, M. Brune, and S. Haroche, *Phys. Rev. A* **86**, 032120 (2012).
- [16] B. Zhu, B. Gadway, M. Foss-Feig, J. Schachenmayer, M. L. Wall, K. R. A. Hazzard, B. Yan, S. A. Moses, J. P. Covey, D. S. Jin, J. Ye, M. Holland, and A. M. Rey, *Phys. Rev. Lett.* **112**, 070404 (2014).
- [17] Y.-J. Han, Y.-H. Chan, W. Yi, A. J. Daley, S. Diehl, P. Zoller, and L.-M. Duan, *Phys. Rev. Lett.* **103**, 070404 (2009).
- [18] Y. S. Patil, S. Chakram, and M. Vengalattore, *Phys. Rev. Lett.* **115**, 140402 (2015).
- [19] L. S. Schulman, *Phys. Rev. A* **57**, 1509 (1998).
- [20] J. G. Muga, J. Echanobe, A. del Campo, and I. Lizuain, *J. Phys. B: At. Mol. Opt. Phys.* **41**, 175501 (2008).
- [21] A. Kofman and G. Kurizki, *Nature* **405**, 546 (2000).
- [22] M. Grigorescu, *Physica A256* (1998) 149-162 **256**, 149 (1998).
- [23] J. Li, A. K. Harter, J. Liu, L. de Melo, Y. N. Joglekar, and L. Luo, *Nat. Commun.* **10**, 855 (2019).
- [24] Y. N. Joglekar and A. K. Harter, *Photon. Res.* **6**, A51 (2018).
- [25] R. d. J. León-Montiel, M. A. Quiroz-Juárez, J. L. Domínguez-Juárez, R. Quintero-Torres, J. L. Aragón, A. K. Harter, and Y. N. Joglekar, *Commun. Phys.* **1**, 88 (2018).
- [26] M. Naghiloo, M. Abbasi, Y. N. Joglekar, and K. W. Murch, *Nat. Phys.* **15**, 1232 (2019).
- [27] A. Guo, G. J. Salamo, D. Duchesne, R. Morandotti, M. Volatier-Ravat, V. Aimez, G. A. Siviloglou, and D. N. Christodoulides, *Phys. Rev. Lett.* **103**, 093902 (2009).
- [28] C. E. Rüter, K. G. Makris, R. El-Ganainy, D. N. Christodoulides, M. Segev, and D. Kip, *Nat. Phys.* **6**, 192 (2010).
- [29] A. Regensburger, C. Bersch, M.-A. Miri, G. Onishchukov, D. N. Christodoulides, and U. Peschel, *Nature* **488**, 167 (2012).
- [30] W. D. Heiss, *J. Phys. A: Math. Theor.* **45**, 444016 (2012).
- [31] J. Schindler, A. Li, M. C. Zheng, F. M. Ellis, and T. Kottos, *Phys. Rev. A* **84**, 040101 (2011).
- [32] S. Assaworrorarit, X. Yu, and S. Fan, *Nature* **546**, 387 (2017).
- [33] M. Chitsazi, H. Li, F. M. Ellis, and T. Kottos, *Phys. Rev. Lett.* **119**, 093901 (2017).
- [34] B. Peng, S. K. Ozdemir, F. Lei, F. Monifi, M. Gianfreda, G. L. Long, S. Fan, F. Nori, C. M. Bender, and L. Yang, *Nat. Phys.* **10**, 394 (2014).

- [35] H. Xu, D. Mason, L. Jiang, and J. Harris, *Nature* **537**, 80 (2016).
- [36] M. Brandstetter, M. Liertzer, C. Deutsch, P. Klang, J. Schöberl, H. E. Türeci, G. Strasser, K. Unterrainer, and S. Rotter, *Nat. Commun.* **5**, 4034 (2014).
- [37] J. Xu, Y.-X. Du, W. Huang, and D.-W. Zhang, *Opt. Express* **25**, 15786 (2017).
- [38] L. Xiao, X. Zhan, Z. Bian, K. Wang, X. Zhang, X. Wang, J. Li, K. Mochizuki, D. Kim, N. Kawakami, *et al.*, *Nat. Phys.* **13**, 1117 (2017).
- [39] Y. Wu, W. Liu, J. Geng, X. Song, X. Ye, C.-K. Duan, X. Rong, and J. Du, *Science* **364**, 878 (2019).
- [40] Y.-R. Zhang and H. Fan, *Sci. Rep.* **5**, 11509 (2015).
- [41] A. Z. Chaudhry, *Sci. Rep.* **6**, 29497 (2016).
- [42] A. Z. Chaudhry and J. Gong, *Phys. Rev. A* **90**, 012101 (2014).
- [43] W. Wu and H. Q. Lin, *Phys. Rev. A* **95**, 042132 (2017).
- [44] Y. N. Joglekar, R. Marathe, P. Durganandini, and R. K. Pathak, *Phys. Rev. A* **90**, 040101 (2014).
- [45] W. Wu and H.-Q. Lin, *Phys. Rev. A* **95**, 042132 (2017).
- [46] Z. Zhou, Z. Lü, H. Zheng, and H.-S. Goan, *Phys. Rev. A* **96**, 032101 (2017).
- [47] Y. Li, X. Chen, and M. P. A. Fisher, *Phys. Rev. B* **98**, 205136 (2018).
- [48] H. Fröml, C. Muckel, C. Kollath, A. Chiocchetta, and S. Diehl, [arXiv:1910.10741](https://arxiv.org/abs/1910.10741).